

~~BAF~~  
~~FJH~~

**RB-81**

**PHOTOELECTRIC EMISSION**

GC CD ES JS PS  
JD VC IGY LS MF  
**RECEIVED**  
DEC 18 1956  
G. R. TUBE ENGINEERING  
NOTE FILE DISCUSS  
ANS RETURN LOG



**RECEIVED**  
DEC 20 1956  
G. R. TUBE ENGINEERING - 2

**RADIO CORPORATION OF AMERICA  
RCA LABORATORIES  
INDUSTRY SERVICE LABORATORY**

RB-81

I OF 11 PAGES

DECEMBER 3, 1956

**RADIO CORPORATION OF AMERICA**  
**RCA LABORATORIES**  
**INDUSTRY SERVICE LABORATORY**

**RB-81**

**PHOTOELECTRIC EMISSION**

This report is the property of the Radio Corporation of America and is loaned for confidential use with the understanding that it will not be published in any manner, in whole or in part. The statements and data included herein are based upon information and measurements which we believe accurate and reliable. No responsibility is assumed for the application or interpretation of such statements or data or for any infringement of patent or other rights of third parties which may result from the use of circuits, systems and processes described or referred to herein or in any previous reports or bulletins or in any written or oral discussions supplementary thereto.



This bulletin reviews the fundamental concepts of photoelectric emission and the experimental methods for measuring parameters, such as yield curves, emission velocity etc. Properties and activation processes of the most important practical photocathodes are described.

### Introduction

Photoelectric emission occurs when the absorption of a photon leads to the ejection of an electron from the absorbing material into the vacuum. This emission may be thought of as a three-step process consisting of: (1) the absorption of a photon by an electron, (2) the motion of the excited electron to the vacuum interface of the solid, and (3) the escape of the electron over the potential barrier at the surface of the solid. In addition to its practical applications, photoemission is of interest because of the information it may give about these processes. Most of the experimental results to date have aided our understanding of the 1st and 3rd steps in the process while very little has been learned about the 2nd step. The mechanism of these three steps differs in many respects for metals, on the one hand, and semiconductors or insulators<sup>1</sup>, on the other hand, because of the difference in band structure in these two classes of materials. These differences will be outlined briefly because they are of importance for both the techniques and the interpretation of experimental work.

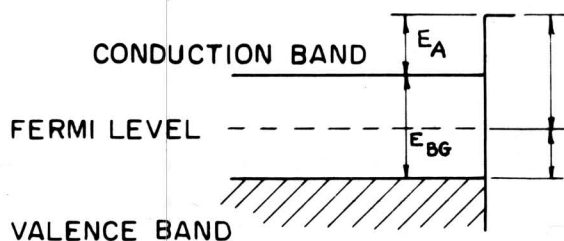
In a metal, provided the photon energy does not greatly exceed the threshold energy, the photoelectrons must originate in the conduction band relatively close to the Fermi level. In general, such unbound electrons are unable to absorb photons because of the need for the conservation of momentum. However, near the surface momentum may be conserved by interaction with the potential gradient in this region.<sup>2</sup> While radiation near the threshold can thus only produce photoelectrons near the surface, there is evidence that for higher energy photons the photoelectrons arise from optical absorption in the bulk of the material.<sup>3,4</sup> In semiconductors, the photons interact with bound electrons, i.e., the photoelectrons originate in the valence band or in impurity states, so that this problem of conservation of momentum does not arise.

Metals and semiconductors also differ in step (2), the mechanism by which an excited electron loses energy in moving through the solid. In a metal, the excited electron may lose energy by lattice scattering and by scattering with the conduction band electrons. The latter loss process may be relatively large and thus may prevent electrons excited deep in the material from reaching the surface with sufficient energy to escape.

In a semiconductor, the principal sources of energy loss are lattice scattering and the excitation of valence band electrons into the conduction band. However, the latter process can only take place when the kinetic energy of the electron exceeds the energy corresponding to the band gap. If the electron energy falls short of the band gap energy, the excited electron will lose energy only relatively slowly through lattice scattering.<sup>5</sup> Thus electrons of sufficiently high energy originating relatively deep<sup>6</sup> in the material can escape provided the electron affinity of the semiconductor is smaller than the band gap energy. This, together with their high optical absorption, may explain why semiconductors have been found to be the most efficient photoemitters.

In addition to the above mentioned differences between metals and semiconductors, another difference becomes apparent when an attempt is made to compare thermionic and photoelectric emission. In a metal, thermionic and photoelectric work functions are identical and defined as the energy difference between Fermi level and vacuum level. In a semiconductor, the thermionic work function is again the energy difference between Fermi and vacuum level. However, there is no longer a universal relationship between thermionic work function and photoelectric threshold since this threshold is determined by the energy difference between the vacuum level and the states with sufficiently high electron densities to produce appreciable photoemission. As can be seen in Fig. 1, the photoelectric threshold will, in general, be greater than the thermionic work function.

\*The material in this bulletin was originally written for a series of volumes entitled METHODS IN EXPERIMENTAL PHYSICS.



(a) Intrinsic semiconductor.

$$\delta = \frac{1}{2} E_{BG}. \text{ Hence, } E_{PE} = \phi + \delta + \frac{1}{2} E_{BG}.$$

( $\delta$  = energy differences between top of valence band and Fermi level.)

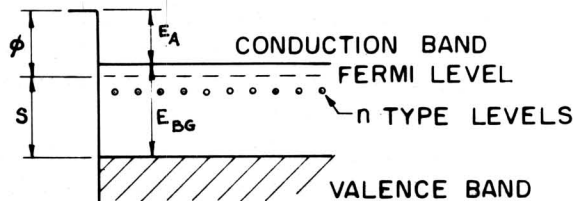
$E_{BG}$  = band gap energy.

$E_{PE}$  = energy corresponding to photoelectric threshold.

$\phi$  = work function.

$E_A$  = electron affinity.)

For a p-type semiconductor the model would be the same except that  $\delta \neq \frac{1}{2} E_{BG}$ .



(b) N-type semiconductor.

Fermi level halfway between impurity levels and conduction band. Assuming only impurity photoelectrons:

$$E_{PE} = \phi + E_{BG} - 8.$$

(A number of other configurations are possible.)

Fig. 1 - Relationships between photoelectric threshold and work function of semiconductors.

### Methods of Measurement

Several parameters may be varied in making emission measurements. The photocurrent may be measured as a function of the wavelength of the incident light, or of the temperature of the emitter at a fixed wavelength, or the energy distribution of the emitted electrons may be measured at a fixed wavelength. Before discussing the various measuring methods, some details are given as to the preparation of the photocathodes.

#### Preparation of Cathode Materials

To obtain meaningful results, it is essential that the emitting surface be extremely clean. Refractory metal

cathodes may be cleaned satisfactorily by heating.<sup>7</sup> In other cases, clean surfaces may be provided by vacuum evaporation of the metal. Special precautions must be taken with metals such as the alkali metals which are unstable in air. They may be provided in a pure form by vacuum distillation or by reduction of a salt in the vacuum. It is also necessary that the pressure in the tube be so low that the gas absorption will not change the surface properties during an experimental run.

The preparation of practical semiconductor photocathodes is a more complex process and will be described in more detail later. Cathodes of a single semiconducting element have been formed by evaporation.<sup>8</sup>

#### Measurement of Spectral Response Curve

In such measurements, the incident radiation is provided by a monochromator. The spectrum has to be very pure because at wavelengths where the photoemitter has low sensitivity, stray light of a more effective spectral range may lead to serious errors. Deficiencies of the monochromator in this respect are often overcome by use of filters which are opaque to the unwanted spectral range. To obtain absolute photocurrent vs incident energy values, the varying energy emitted by the monochromator at different wavelengths has to be normalized by an energy measuring device such as a thermocouple. The photoelectric current is often quite small, necessitating the use of sensitive current measuring methods such as electrometers or chopped light with a-c amplification.

Care must be taken that the applied voltage is large enough to saturate the current but excessive voltage should be avoided. The saturation voltage depends on the geometry of the experimental tube. The ideal geometry consists of a spherical anode surrounding a relatively small emitter at its center. In this case, the saturation voltage is usually less than ten volts. However, other considerations often necessitate much less favorable geometries so that as much as a hundred volts may be required for saturation. In such cases, care must be taken that the results are not confused by the charging of glass surfaces in the tube, space charge, or other effects.<sup>9</sup>

#### Energy Distribution Measurements

There are two general methods<sup>10</sup> by which energy distribution can be determined: (1) retarding potential measurements<sup>11</sup>, and (2) magnetic deflection measurements. In the former case, integral distributions are obtained, i.e., all the electrons of energy above a given minimum value are collected, whereas in the latter case, a differential distribution is obtained, i.e., only the electrons in a velocity range  $\Delta E$  are collected. Because of the

effect of the contact potential difference, it is very important that the work function of the collecting surface (in the case of the retarding potential method) or of the surface of the analyzing chamber facing the photoemitting surface (in the case of magnetic deflection) be uniform and known for the determination of the contact potential difference.

For retarding potential measurements, one can use either plane parallel or spherical geometry. In the plane parallel case, only the component of velocity perpendicular to the surface is measured; whereas in the spherical case, the total energy is measured. For good spherical geometry, the emitter should be as small as possible in comparison to the collector. As Apker et al<sup>7</sup> have pointed out, care must be taken to compensate for the contact potential between the emitter leads and the cathode.

The magnetic analyzers can be designed for either transverse<sup>12</sup> or longitudinal<sup>13</sup> fields. In the former case, the electrons are selected by deflection in a circular path of fixed radius. Here only the component of velocity perpendicular to the emitting surface is measured. However, in the case of longitudinal fields, a component of velocity directed off the normal to the emitting surface is measured. The angle with the normal is determined by the geometry of the system.

### Interpretation of Data

#### Metals

The long wavelength cut-off or threshold of photoemission is of considerable interest since this gives a measure of the minimum energy necessary to remove an electron from the solid. However, due to the lack of an absolutely sharp cut-off, this threshold is not uniquely defined experimentally. In metals, the threshold may be even less sharp than for semiconductors where impurity levels or the valence band provide the photoelectrons rather than the conduction band. However, Fowler<sup>14</sup> has derived a simple theory giving the photoelectric yield curve near the threshold as a function of the energy of the exciting light. To do this, Fowler used Fermi-Dirac statistics and assumed that (1) only those electrons may escape for which the sum of photon energy and that part of the kinetic energy directed perpendicular to the surface is greater than the work function, and (2) the probability of excitation and escape is equal for all electrons for which condition (1) is satisfied. Experimental data may be matched<sup>15</sup> to the Fowler function to give the position of the Fermi level, i.e., the work function of the metal. Copious experimental verification has been obtained for

this theory.<sup>7</sup> DuBridge<sup>15</sup> has extended Fowler's theory so that the value of the work function may be obtained by keeping the wavelength of the exciting light constant and varying the temperature of the sample.

By a method similar to that of Fowler, DuBridge<sup>16</sup> has derived equations to which retarding potential curves obtained from metals near the threshold may be fitted to obtain the work function of the metal. These apply for plane parallel or spherical geometry. However, the Fowler method is usually the simplest for determining work functions of metals; and energy distribution methods are probably more valuable for investigating other aspects of photoemission.<sup>17</sup>

#### Semiconductors

Due to the lack of a precise theory of photoemission from semiconductors, the interpretation of experimental data is much less clear than for metals. If indirect excitation processes such as exciton excitation are not involved, yield curves give a measure of the distribution of filled electron states in the solid and, in particular, the threshold of photoemission gives an estimate of the position of the highest level with a sufficiently large electron density. In cases where the photoemissive electrons originate in the valence band, the threshold may be quite sharp. In such a case, the threshold<sup>18</sup> will give the energy difference,  $E_{PE}$ , between the top of the valence band and the vacuum level. Since photoconductivity and/or absorption measurements may be used to determine the band gap,  $E_{BG}$ , the electron affinity,  $E_A$ , will then be given by

$$E_A = E_{PE} - E_{BG} . \quad (1)$$

Similar arguments may be applied to impurity levels.<sup>19</sup>

Such determinations are usually accurate within a few tenths of an electron volt or less and may provide a simple method of obtaining values for energy band models. Typical data taken from a single tube containing a very thin ( $\approx 400 \text{ \AA}$ )  $K_3Sb$  photocathode is given in Fig. 2.

Apker and his co-workers have extended the use of retarding potential measurements to semiconductors.<sup>8</sup> No attempt will be made here to describe their experimental arrangement other than to mention that they used spherical geometry, but their method of interpreting data will be briefly discussed.

The work function of the semiconducting emitter may be determined by measuring the contact potential difference between emitter and collector. In the absence of any applied voltage, the voltage difference between emitter and collector is the contact potential. Saturation will be reached when the applied voltage cancels out the contact potential. Thus the saturation voltage,  $V_s$ , will be given by:

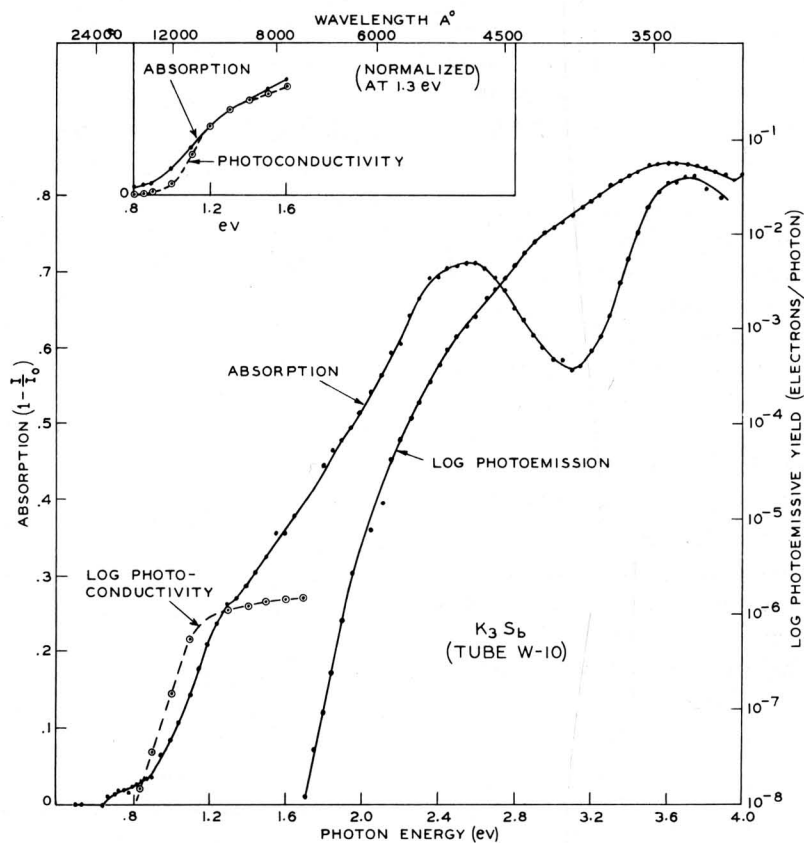


Fig. 2 - Absorption, photoconductivity and photoemission data for  $K_3Sb$ . Absorption and photoconductivity indicate a band gap of about 1.0 eV. Defining photoemissive threshold as the energy at which the photoemissive efficiency falls to  $10^{-8}$  electron/photon, a threshold energy of 1.7 eV is obtained. Equation (1) then gives an electron affinity of 0.7 eV.

$$eV_s = \phi_c - \phi = \text{contact potential difference} \quad (2)$$

where  $\phi_c$  is the work function of the collector and  $\phi$  that of the emitter.

Thus to determine the work function of the emitter, it is necessary to know the work function of the collector. To determine this, the tube was provided with metallic emitters which could be interchanged with the sample under study. Photocurrent could thus be drawn from the metallic emitter and measured as a function of voltage.  $V_o$ , the voltage necessary to stop photocurrent, if the cathode were at 0 degrees K, was determined from this data by DuBridge's<sup>16</sup> method. Since

$$eV_o = h\nu - \phi_c, \quad (3)$$

the work function of the collector could then be determined. The value obtained for  $\phi_c$  by this method may be checked by determining the work function of the metallic emitter through Fowler's method and then determining the saturation voltage and using equation (2) to determine the work function of the emitter. For accuracy in these measure-

ments, the collector must have a uniform work function.

In order to determine the saturation voltage  $V_s$ , it is useful to measure current as a function of the applied voltage  $V$  for a fixed wavelength of light. This data is plotted in the form<sup>8</sup>

$$1 - (1 - I/I_o)^{1/2} \text{ vs } V$$

where  $I$  is the current with voltage  $V$  and  $I_o$  is the saturation current. Such a plot should essentially consist of two straight line portions; one in the retarding potential region increasing with voltage, and one with almost no slope in the saturation region. The intersect of these gives the saturation voltage.

As indicated in Fig. 1,  $\phi$  gives the energy difference between the Fermi level and the vacuum level for any emitter in electronic equilibrium with its surroundings.<sup>20</sup> Neglecting the effect of any structure in the emitting level, the position of the level relative to the Fermi level would be given by

$$eV_s - eV_o' = h\nu - \delta - \phi \quad (4)$$

where  $V_o'$  is the voltage necessary to stop the photocurrent and  $\delta$  is the energy difference between the emitting level and the Fermi level. The photoelectric threshold  $E_{PE}$  will be given by

$$E_{PE} = \delta + \phi.$$

On measuring  $V_o'$ , it is usually necessary to correct for electron emission from other parts of the tube collected by the cathode.<sup>21</sup> As mentioned previously,  $E_{PE}$  may also be obtained from the threshold of the photoemissive yield curve.

However, since the thresholds are not completely sharp for either the yield or retarding potential curves, the accuracy of such methods for determining  $\phi$  is not as great as might be desired. Apker et al<sup>8</sup> have developed a theoretical expression to which either retarding potential or yield curves may be fitted to give  $\phi$ . They have also pointed out that by assuming the probability of escape for an excited electron to be proportional to  $E$ , its kinetic energy on escape, the following relationship should hold:

$$\frac{N(\nu, E)}{E} dE \propto n(\epsilon) S(\nu, \epsilon) d\epsilon$$

where  $N(\nu, E)dE$  is the number of electrons with kinetic energy  $E$ , in the range  $dE$ ,  $n(\epsilon)$  is the density of electronic states at an energy  $\epsilon$ , in the range  $d\epsilon$  and  $S(\nu, \epsilon)$  is the probability of light of frequency  $\nu$  exciting an electron from a state at  $\epsilon$ . The assumptions necessary in these derivations may reduce the accuracy of the method. This technique has been applied to the semi-metals<sup>22</sup> as well as semiconductors and should be applicable to insulators if they are in electronic equilibrium with their surroundings.<sup>20</sup>

## Practical Photocathodes

### Introduction

Photocathodes can be formed as opaque layers with the light incident on the vacuum interface or as semi-transparent layers with the light usually incident on the interface between cathode and (transparent) supporting material. Opaque cathodes can be formed in arbitrary thickness, either directly on the glass wall of an evacuated tube or on a conducting base material such as a solid metal electrode or a conducting coating on glass or mica. For semi-transparent cathodes, the thickness is critical because the layer must be thick enough to absorb most of the incident light, but thin enough for photoelectrons

originating near the cathode-glass interface to have a high probability of escape. The optimum thickness is usually in the range of 100 atomic layers.

Despite the more critical activation process, semi-transparent cathodes are preferred for devices such as multiplier tubes and television pickup tubes because they simplify light and electron optics. They are also required for the study of light absorption in photoemitting materials. Contrary to expectation, it has been found that light incident on the glass interface of a semi-transparent cathode may release more photoelectrons than light incident on the vacuum interface. This has been attributed to the complex mechanism of light absorption if the wavelength of the light is greater than the film thickness.

Photoemitters with useful quantum efficiency have several features in common: First, they are semiconductors. Second, they all contain alkali metals. Third, in all compounds containing a single alkali metal the threshold wavelength increases in the series  $Li \rightarrow Na \rightarrow K \rightarrow Rb \rightarrow Cs$  so that the  $Cs$  compound is always the most sensitive to visible light. In the following summary of the forming process, photoelectric characteristics, and other properties of photocathodes, attention is confined in most cases to the  $Cs$  compound and to semi-transparent cathodes because the activation process and properties for the compounds with other alkali metals and for opaque cathodes are basically similar. For more details on the formation of photocathodes, the reader is referred to references 23 and 24.

### The Antimony-Cesium (Sb-Cs) Cathode

Since 1936<sup>25</sup> many photoemissive materials have been found which have the common characteristic that they are semiconducting intermetallic compounds of alkali metals with metals of the 4th, 5th or 6th group of the periodic system. Outstanding among these materials is the  $Sb$ - $Cs$  cathode because it has high photosensitivity, is simple to produce and has been the subject of numerous experimental studies aimed at a better understanding of the photoelectric mechanism.

Formation. The formation of a  $CsSb$  cathode as well as of all subsequent cathodes requires a vacuum in the range of  $10^{-6}$  mm of  $Hg$  or below. The first step in the process is the evaporation of an  $Sb$  layer which is monitored by measuring the transmission of white light through the layer. The evaporation is stopped when the transmission has fallen by between 20 and 50 percent. The tube is then heated to between 120 and 150 degrees C and the layer is exposed to  $Cs$  vapor. Since alkali metals oxidize at once upon exposure to air, the  $Cs$  required for the activation is usually produced within the evacuated tube itself or in an attached side-tube. This is conveniently done by filling a nickel pellet with an intimate mixture of a  $Cs$  salt and a reducing agent, for instance, 1 part of  $Cs_2CrO_4$



powder with 4 parts of pure *Si* or *Zr* powder.<sup>26</sup> *Cs* is evolved from this mixture when it is heated to temperatures greater than 700 degrees C.

With the tube and the *Sb* layer held at a temperature of 120 to 150 degrees C, the *Cs* readily reacts with *Sb* to form the photosensitive compound. This reaction is accompanied by three characteristic phenomena. First, the *Sb* layer loses its metallic appearance and assumes a red color in transmitted light. Second, the resistance of the layer rises rapidly by several orders of magnitude above that of the original *Sb* layer, indicating the formation of a semiconductor. Third, white light produces photoelectric emission which rises to a peak and then drops rapidly with continued exposure to *Cs*. The activation process is usually followed by monitoring the photoemission. When the photoemission passes over the peak, the introduction of *Cs* is stopped and the baking process is then continued until the photocurrent reaches a constant peak value. After cooling the tube, the sensitivity, particularly for red light, can be further improved by carefully exposing the cathode to oxygen until the photoemission again reaches a peak. The  $O_2$  is conveniently introduced by heating, in a side-tube, a salt such as  $KMnO_4$  or  $KClO_3$  to the temperature at which it releases oxygen.

**Properties.** Typical response curves of *Sb-Cs* cathodes before and after superficial oxidation are shown in Fig. 3. The most important features of the oxidized cathode are the high quantum efficiency of up to 0.20 electron per incident photon at wavelengths below approximately 4200 Å and a practical threshold wavelength of approximately 7000 Å. For practical purposes the sensitivity of a photocathode is often given in microamperes per lumen ( $\mu a/l$ ). Since the lumen is based on the color distribution of a tungsten lamp at 2870 degrees K, the  $\mu a/l$  value is a measure of the response to this type of source. *Sb-Cs* cathodes have usually a sensitivity of 30 to 60  $\mu a/l$ , and occasionally as high as 90  $\mu a/l$ .

In the detection of very low light levels, the thermionic emission of a cathode at room temperature is an undesirable feature because it may limit the signal-to-noise ratio. The thermionic emission of the *Sb-Cs* cathode is usually below  $10^{-14}$  amp/cm<sup>2</sup>.

The reproducible performance of the *Sb-Cs* photocathode made it appear likely that the material should have a well defined chemical composition. Quantitative studies<sup>27</sup> suggested the stoichiometric formula  $Cs_3Sb$ . However, with present analytical methods, it is not possible to detect minute excess amounts of *Sb* or *Cs* within the cathode material and/or adsorbed to the surface. It may well be that just such a small excess of one of the components is of significance in the photoelectric mechanism.

Values of the band gap energy have been reported<sup>28</sup> as determined from measurements of light absorption, photo-

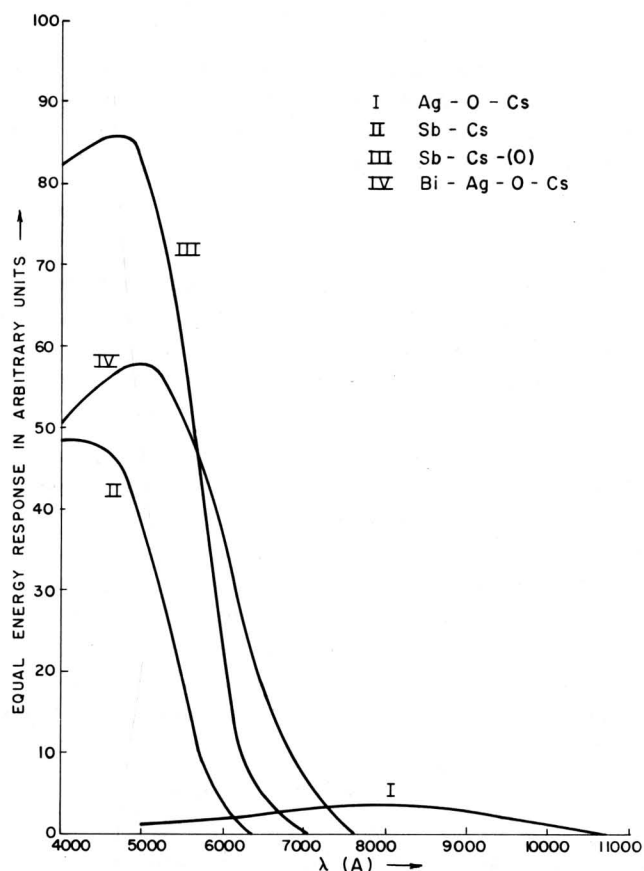


Fig. 3 - Spectral response curves of commonly used photocathodes.

conductivity and  $\log \sigma$  vs  $1/T$  curves. The electron affinity has been computed from photoemission thresholds and attempts have also been made to measure the thermionic work function. Finally, measurements of the thermoelectric<sup>29</sup> and Hall<sup>30</sup> effect have been made to establish the sign of the current carriers in  $Cs_3Sb$ ; at present the evidence is in favor of *p*-type conduction.

#### Miscellaneous Cathodes of the *Sb-Cs* Type

Under this heading are briefly reviewed other photoemitters which are semiconducting stoichiometric compounds of an alkali metal with another metal, but differ from  $Cs_3Sb$  by having lower sensitivity in the visible spectrum. The *Sb* may be replaced by metals of the 4th group (*Si*, *Ge*, *Sn*, *Pb*), the 5th group (*As*, *Bi*) and the 6th group (*Se*, *Te*). Two of these compounds deserve special mention:  $Cs_3Bi$  because, among the cathodes not containing *Sb*, it comes closest to  $Cs_3Sb$  in sensitivity to visible light, though its quantum efficiency is down by a factor of about ten;<sup>25</sup>  $Cs_2Te$  because it has very high quantum efficiency in the ultra-violet (up to 30 percent) though it does not appear to have found practical application up to the present.<sup>31</sup> As mentioned in the introduction, photo-

cathodes may also be formed by replacing Cs with other alkali metals. The response curves of  $K_3Sb$  and  $Na_3Sb$  are shown in Fig. 4.

*Multi-alkali Cathodes*

Whereas Cs is superior to other alkali metals in all types of cathodes, it has been found<sup>32</sup> that the combination of two or more alkali metals with antimony may in some cases produce higher sensitivity than Sb with any one of these alkali metals. This "multi-alkali effect" has been definitely established for two cathodes of the general formulae  $Sb-K-Na$  and  $Sb-K-Na-Cs$ . The formation process for these cathodes is essentially similar to that of the  $Cs_3Sb$  cathode but the introduction of the alkali metals has to be carefully controlled because the ratio in the final layer is critical.

The spectral response curve for  $Sb-K-Na$  is shown in Fig. 4 and comparison with the curves for the corresponding single alkali cathodes  $K_3Sb$  and  $Na_3Sb$  shows the magnitude of the multi-alkali effect. The sensitivity of the  $Sb-K-Na$  cathode is similar to that of superficially oxidized  $Cs_3Sb$  but it has the advantage of much lower thermionic emission at room temperature.

The response curve of an  $Sb-K-Na-Cs$  cathode is shown in Fig. 4 and covers the visible spectrum more effectively than any other emitter. The thermionic emission at room

temperature, despite the longer threshold wavelength, is not larger than that of superficially oxidized  $Cs_3Sb$ .

There is no explanation for the multi-alkali effect but measurements of light absorption, photoconductivity and chemical composition make it certain that the  $Sb-K-Na-Cs$  cathode is basically an  $Sb-K-Na$  cathode whose electron affinity is reduced by a surface layer of Cs; there are also indications<sup>33</sup> that the improvement in red response of the  $Sb-K-Na-Cs$  cathode over the  $Cs_3Sb$  cathode is caused by a lower value of the band gap energy, while the high yield of the  $Sb-K-Na$  cathode, compared with  $K_3Sb$  and  $Na_3Sb$ , is associated with a lowering of the electron affinity.

*The Silver-Oxygen-Cesium (Ag-O-Cs) Cathode*

**Formation.** The first step in the preparation of an Ag-O-Cs cathode is the formation of a silver base. This can be produced in a number of ways, such as electroplating, chemical deposition or evaporation. The last method is preferable because it produces the cleanest and most uniform surface; it also is the only method by which a semi-transparent cathode of controlled thickness can be made. The silver base is oxidized by exposure to a glow discharge in 0.1 to 1 mm pressure of oxygen. The oxidation is accompanied by a characteristic color change which allows accurate control of the process. The colors go through golden-yellow to blue and then green. The best results are obtained if the oxidation is stopped at the blue color. (This applies to opaque cathodes; semi-transparent silver layers are completely oxidized resulting in almost 100 percent transparency.)

After the tube has been evacuated again, the silver oxide is exposed to Cs vapor and at about 150 degrees C a reaction takes place at once. As soon as the photoemission passes through a maximum, the introduction of Cs is stopped and the tube is held at the indicated temperature until the photocurrent reaches a stable maximum value. It has been found<sup>34</sup> that higher sensitivity is obtained by additional evaporation of a small amount of Ag, followed by another baking process to maximum photocurrent.

**Properties.** A typical color response curve of an Ag-O-Cs cathode is shown in Fig. 3. The maximum quantum efficiency in the visible and infrared is only 0.005 electron per photon at 8500 A, but the threshold wavelength beyond 12,000 A makes this cathode valuable for infrared work; in fact, this is the only known photoemitter with useable infrared response. The total sensitivity is 30 to 50  $\mu a/l$ . The thermionic emission at room temperature varies over a wide range ( $10^{-13}$  to  $10^{-9}$  amp/cm<sup>2</sup>) even among cathodes with similar photoelectric behavior, but  $10^{-11}$  amp/cm<sup>2</sup> can be considered an average value.

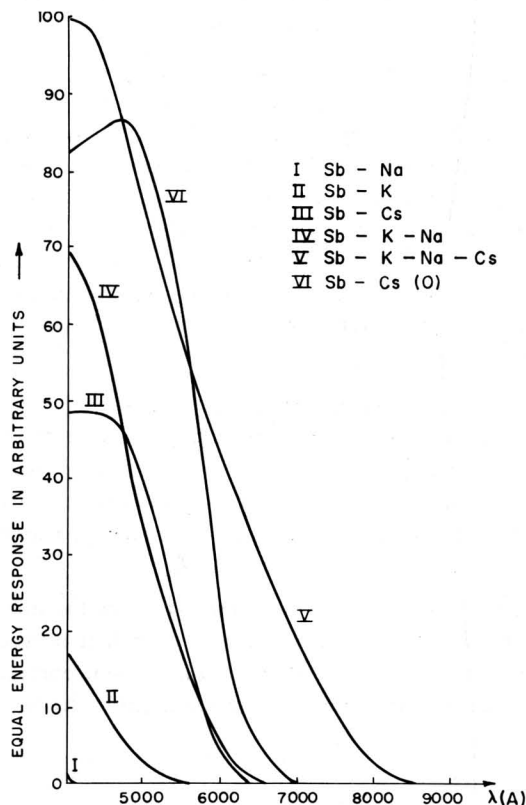


Fig. 4 - Spectral response curves of alkali metal-antimony photocathodes.

TABLE I

Material	Code Number	$\lambda_{(peak)}$	Maximum Quantum Efficiency at $\lambda_{(peak)}$	$\lambda_0$ (1% of peak) in A	Maximum $\mu a/l$	Average Thermionic Emission at Rm. Temp. in amp/cm <sup>2</sup>
Sb-Cs(O) (opaque)	S-4	4,000	.20	7,000	120	$10^{-14}$
Sb-Cs		4,500	.10	6,500	25	$< 10^{-14}$
Sb-Cs(O)	S-11	4,500	.20	7,000	90	$10^{-14}$
Ag-O-Cs	S-1	8,500	.0005	12,000	50	$10^{-11}$
Bi-Ag-O-Cs	S-10	4,500	.10	7,500	90	$10^{-13}$
Sb-K		3,500			5	
Sb-Na		2,700			$< .1$	
Sb-K-Na		$\approx 3,700$	$\approx .25$	6,200	60	$< 10^{-16}$
Sb-K-Na-Cs		$\approx 4,500$	$\approx .25$	8,500	210	$10^{-14}$

Despite a great amount of experimental work, the mechanism of the Ag-O-Cs cathode is little understood. It is only known that the reaction of silver oxide with Cs leads to cesium oxide mixed with Ag, but there is no explanation for the low quantum efficiency nor for the fact that the silver cannot be replaced by any other metal.

#### *The Bismuth-Silver-Oxygen-Cesium (Bi-Ag-O-Cs) Cathode*

The absence of red response in the Cs<sub>3</sub>Sb cathode and the low efficiency of the Ag-O-Cs cathode in the visible range led to unsuccessful attempts at combining these two materials. However, it was found<sup>35</sup> that if Sb in this combination is replaced by Bi, a cathode can be produced which approaches in its properties the desired compromise.

**Formation.** The first step of the process consists of the evaporation of a thin Bi layer with about 60 percent light transmission. This is followed by the evaporation of Ag until the transmission is reduced to about 50 percent. This bismuth-silver layer is then oxidized by a discharge in oxygen or simply by exposure to oxygen until the transmission has increased again to about 55 percent. Finally,

the layer is activated with Cs at approximately 150 degrees C until maximum sensitivity is obtained.

**Properties.** A typical color response curve is shown in Fig. 3. Whereas the peak quantum efficiency is lower than for Cs<sub>3</sub>Sb, the drop toward longer wavelengths is more gradual so that the whole visible range is covered. The total sensitivity is usually 30 to 60 and up to 90  $\mu a/l$ . The cathode is particularly suited for applications where panchromatic response is required<sup>36</sup> (television, spectroscopy). The thermionic emission at room temperature is approximately  $10^{-13}$  amp/cm<sup>2</sup>, i.e., about ten times larger than for Cs<sub>3</sub>Sb.

Nothing is known about the mechanism of this very complex photoemitter. In particular, it is puzzling why Bi in this combination is better than Sb, by contrast with the superiority of the Cs<sub>3</sub>Sb cathode over the Cs<sub>3</sub>Bi cathode. As in the case of the Ag-O-Cs cathode, there is no explanation for the function of the Ag.

The most important characteristics of the described photocathodes are summarized in Table I. It must be emphasized that the values for  $\lambda_{(peak)}$ ,  $\lambda_0$  and, particularly, for thermionic emission vary considerably from tube to tube.

*A. H. Sommer*

A. H. Sommer

*W. E. Spicer*

W. E. Spicer

## References

1. All the statements in this bulletin concerning semi-conductors apply also to insulators and hereafter insulators will not be mentioned separately.
2. I. Tamm and S. Schubin, *Z. f. Physik* **68**, 97 (1931).
3. R. J. Cashman and E. Bassoe, *Phys. Rev.* **55**, 63 (1939).
4. Very high quantum yields have been reported for metals in the vacuum ultra-violet region. See W. C. Walker, N. Wainfan and G. L. Weissler, *J. Appl. Phys.* **26**, 1366 (1955).
5. P. A. Wolff, *Phys. Rev.* **95**, 1415 (1954).
6. J. A. Burton, *Phys. Rev.* **72**, 531 (1947).
7. See, for example, L. Apker, E. Taft and J. Dickey, *Phys. Rev.* **73**, 46 (1948).
8. L. Apker, E. Taft and J. Dickey, *Phys. Rev.* **74**, 1462 (1948).
9. J. S. Preston and G. W. Gordon-Smith, *Brit. J. of Appl. Phys.* **6**, 329 (1955); G. A. Boutry and P. Gillod, *Phil. Mag.* **28**, 163 (1939).
10. For an earlier discussion of these methods see: A. L. Hughes and L. A. DuBridge, PHOTOELECTRIC PHENOMENA, McGraw-Hill, New York, (1932).
11. Other types of electrostatic analyzers are possible. See A. L. Hughes, V. Rojansky and J. H. McMillen, *Phys. Rev.* **34**, 284 (1929).
12. H. R. Philipp, Thesis Univ. of Missouri (1954) (to be published in *Phys. Rev.*); A. R. Hutson, *Phys. Rev.* **98**, 889 (1955).
13. R. Kollath, *Phys. Z.* **41**, 576 (1940).
14. R. H. Fowler, *Phys. Rev.* **38**, 45 (1931).
15. A table giving values of Fowler's function has been published by DuBridge: L. A. DuBridge, *Phys. Rev.* **39**, 108 (1932).
16. L. A. DuBridge, *Phys. Rev.* **43**, 727 (1933).
17. See, for example, J. Dickey, *Phys. Rev.* **81**, 612 (1951).
18. In the absence of theoretical definition, the threshold must be defined as the photon energy at which the yield has dropped to an arbitrary value, e.g.,  $10^{-8}$  electron/photon.
19. H. B. DeVore and J. W. Dewdney, *Phys. Rev.* **83**, 805 (1951).
20. L. Apker and E. Taft, *Phys. Rev.* **82**, 814 (1951).
21. S. S. Prilezaev, *J. Tech. Phys. USSR* **9**, 1439 (1939). (In Russian)
22. L. Apker, E. Taft and J. Dickey, *Phys. Rev.* **76**, 270 (1949).
23. V. K. Zworykin and E. G. Ramberg, PHOTOELECTRICITY AND ITS APPLICATIONS, John Wiley, New York (1949).
24. A. H. Sommer, PHOTOELECTRIC TUBES, John Wiley, New York (1951).
25. P. Görlich, *Z. f. Phys.* **101**, 335 (1936).
26. J. H. de Boer, *Z. anorg. Chem.* **191**, 113 (1930).
27. A. H. Sommer, *Proc. Phys. Soc.* **55**, 145 (1943).
28. G. Wallis, *Annalen der Physik* **17**, 401 (1956). This paper contains copious references to earlier work.
29. T. Sakata, *J. Phys. Soc. Japan* **8**, 125, 272 (1953).
30. T. Sakata, *J. Phys. Soc. Japan* **9**, 1030 (1954).
31. E. Taft and L. Apker, *J. Opt. Soc. Am.* **43**, 81 (1953).
32. A. H. Sommer, *Rev. Scient. Instr.* **26**, 725 (1955).
33. W. E. Spicer, *Phys. Rev.* (in press).
34. S. Asao, *Proc. Phys. Math. Soc. Japan* **22**, 448 (1940).
35. A. H. Sommer, U. S. Patent No. 2,285,062 (1942).
36. However, it may eventually be superseded by the Sb-K-Na-Cs cathode when the latter reaches the stage of commercial manufacture.

